Supplementary Figure 1: Determination of $H_2{}^{18}O$ injection and mixing kinetics

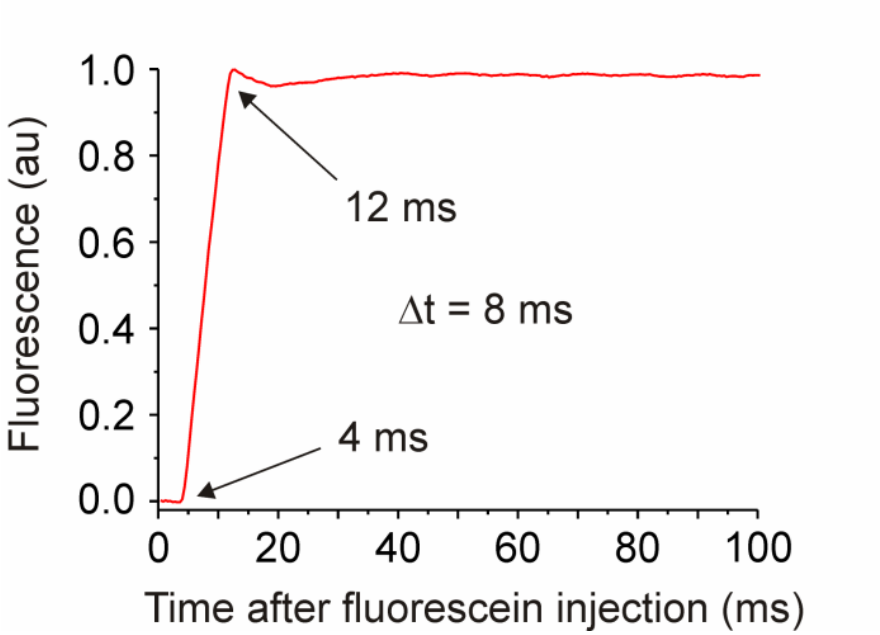

Supplementary Figure 1: The red line shows the rise of fluorescence caused by the injection and mixing of a fluorescein solution (30µM, 40µL) into the MIMS cell pre-filled with a buffer solution (0.1 M Tris pH 8.0, 165µL). The fluorescein was excited by a LED lamp (Luxeon V-Star blue, 1W) via a band pass filter (Newport 470 nm – 495 nm) and one branch of a bifurcated optical fiber. The resulting fluorescence of fluorescein (λ_{ex} 490 nm; λ_{em} 525 nm) was collected via the second branch of the bifurcated optical fiber and a second band pass filter (Newport 520 nm – 547 nm). A photodiode (Hamamatsu S-2281/C9329) was used to convert the fluorescence into a voltage signal, which was recorded with an oscilloscope. The data show that after the injection trigger a dead time of 4-6 ms occurred, followed by an almost linear increase of the signal to a steady plateau that was reached after 8 ms. For the fits of the water exchange kinetics the above mixing kinetics were approximated by a 6 ms delay followed by a mono-exponential rise with a rate of $k_{mix} = 233\ s^{-1}$.

Supplementary Figure 2: Sensitivity of MIMS experiments

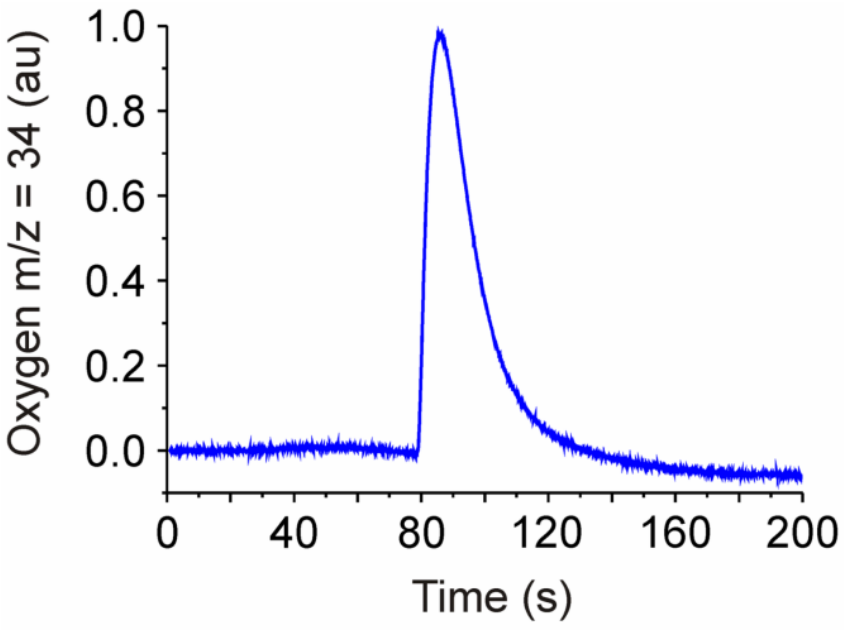

Supplementary Figure 2: $^{16}O^{18}O$ (m/z = 34) signal induced by three flashes given to dark-adapted *T. elongatus* cores at natural $H_2{}^{18}O$-enrichment. Experimental conditions were identical to those in Figure 3C. No smoothing was applied. The excellent S/N of the three flash-induced $^{16,18}O_2$ yield demonstrates that our finding of arrested water exchange in the $S_3Y_Z^{\bullet}$ is not a negative result, i.e. that we are not missing a signal. Instead, we positively measure that the isotopic composition of the dioxygen produced in the experiments displayed in Figure 3 is of natural abundance.

Supplementary Figure 3: Flash-induced O_2 oscillation pattern of a Sr/I-PSII

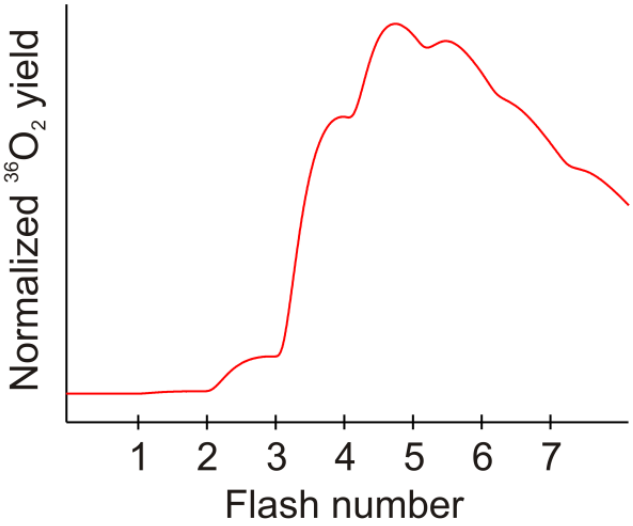

Supplementary Figure 3: Flash-induced O_2 oscillation pattern of a Sr/I-PSII core preparation in absence of added exogenous acceptors as measured with our MIMS set up at a flash frequency of 0.05 Hz. The pronounced maximum of O_2 evolution in the 3rd flash and the large ratio of the O_2-yield of the 3rd flash to that of the 4th flash attest that the mechanism of water exchange occurs with good efficiency in the Sr/I PSII samples. The fast disappearance of the oscillation thereafter is due to the lack of exogenous electron acceptors (not added since good acceptors such as phenyl-para-benzoquinone have to be dissolved in organic solvents, which interfere with the mass spectrometric detection of O_2 and CO_2).

Supplementary Figure 4: Flash-induced pH changes assessed via the absorption changes of bromocresol purple at 575 nm

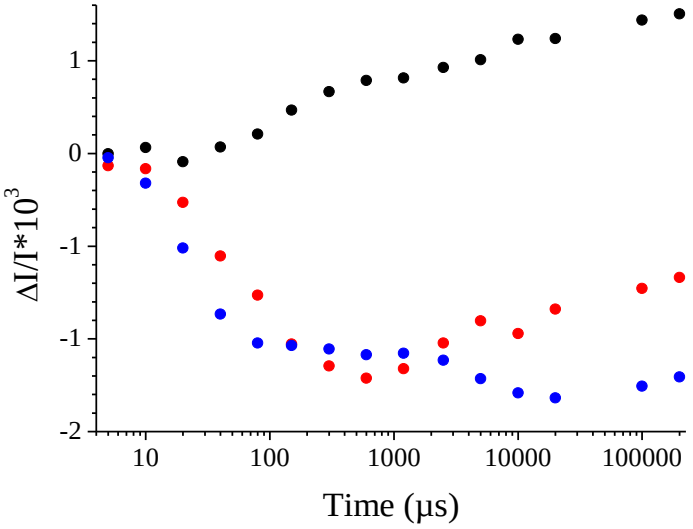

Supplementary Figure 4: Time-courses of the absorption changes at 575 nm after the first flash (black), the second flash (red) and the third flash (blue) given to a dark-adapted Sr/Br-PSII sample in the presence of bromocresol purple.

Supplementary Figure 5: Average flash-induced absorption changes at 575 nm

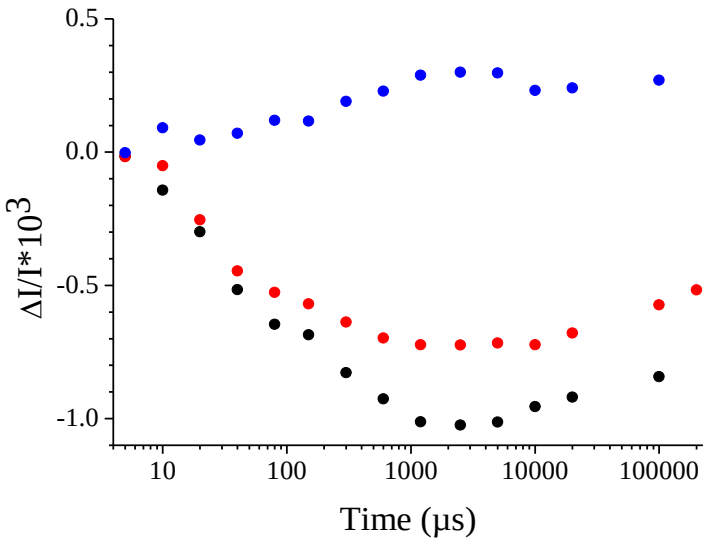

Supplementary Figure 5: Average of the time-courses of the absorption changes at 575 nm after the first four flashes (red points) and after the 35th to 40th flashes (black points). The blue trace is the difference red-minus-black.

Supplementary Figure 6: Apparent proton uptake after each flash

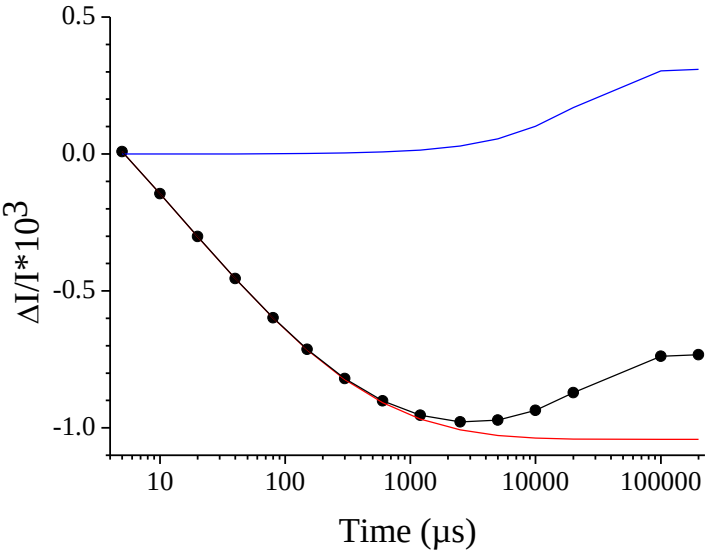

Supplementary Figure 6: Average of the time-courses of the absorption changes at 575 nm after the 35th to 40th flashes (full black circles). The continuous black line joins the experimental data points. The red line is a fit of the experimental data points that reflects the release of one proton. The blue trace is the difference red-minus-black and reflects an apparent proton uptake that occurs after each flash.

Supplementary Figure 7: Corrected flash-induced absorption changes at 575 nm

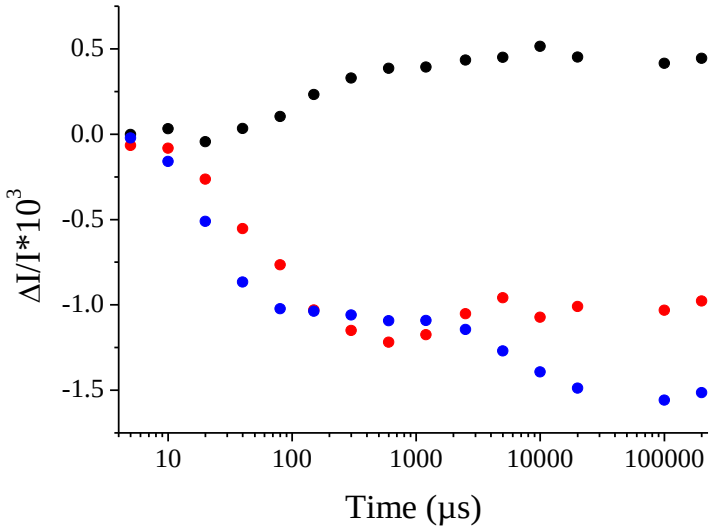

Supplementary Figure 7: Corrected time courses of the absorption changes at 575 nm measured after the first flash (black), the second flash (red) and the third flash (blue) given to dark-adapted Sr/Br-PSII samples. The traces were obtained from the data displayed in Supplementary Figure 4 by subtracting the apparent proton uptake which occurs in all S state transitions (blue line in Supplementary Figure 6).

Supplementary Figure 8: Fit of Proton release kinetics after the 3rd flash

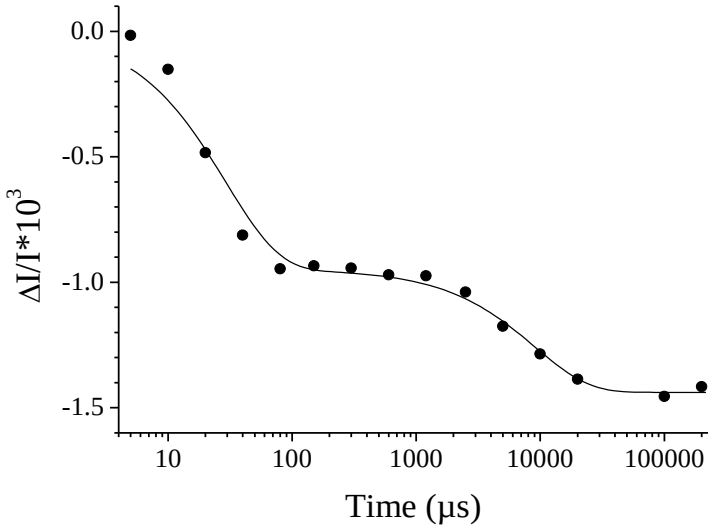

Supplementary Figure 8: Replot of the time course of the corrected absorption change at 575 nm observed after the third flash (full circles; compare blue symbols in Supplementary Figure 7;) and result of the fitting procedure (continuous line) by using a two exponential decay with $t_{1/2}$ = 22 µs for the fast phase and $t_{1/2}$ = 6.3 ms for the slow phase.

Supplementary Figure 9: Oscillation pattern of flash-induced absorption changes at 575 nm

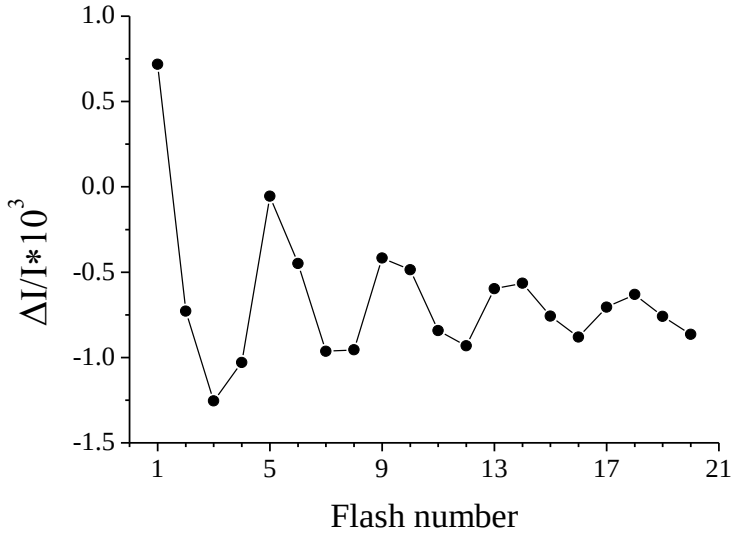

Supplementary Figure 9: Sequence of the amplitudes of the absorption changes at 575 nm measured 100 ms after the indicated number of flashes (full circles joined by straight lines). The measurements were done during a train of saturating flashes (spaced 200 ms apart) given to dark-adapted Sr/Br-PSII.

Supplementary Figure 10: Oscillation pattern of flash-induced proton release

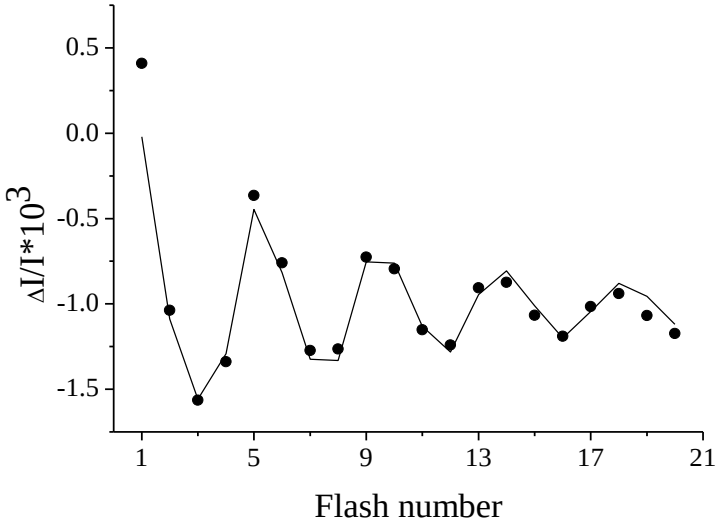

Supplementary Figure 10: Corrected sequence of the amplitudes of the absorption changes at 575 nm measured 100 ms after the indicated number of flashes (black symbols). These are the same data as in the Supplementary Figure 9, but after subtraction of the non-oscillating contribution determined in Supplementary Figure 6. The continuous line represents the result of a fit in which the first flash was excluded.

Supplementary Note 1

Proton release during $S_3^+Y_Z^\bullet \rightarrow S_0Y_Z$ transition in Sr/Br samples

During the turnover of the Kok cycle the increase in charge resulting from electron abstraction from the Mn_4CaO_5 cluster is compensated for by proton release, thus keeping the redox potential of the catalytic center below that of $Y_Z^\bullet/Y_Z$ [1-3]. There is a broad consensus that at pH 6.5 the stoichiometry for the proton release from the water oxidizing complex (WOC) into the bulk is close to 1, 0, 1, 2 protons in the $S_0Y_Z \rightarrow S_1Y_Z$, $S_1Y_Z \rightarrow S_2^+Y_Z$, $S_2^+Y_Z \rightarrow S_3^+Y_Z$ and $S_3^+Y_Z \rightarrow S_0Y_Z$ transitions, respectively, e.g. ref[4-9]. Several different approaches concurred in establishing this: sensitive glass electrodes[5,8], absorption changes of pH-responding dyes[4,6,9] and isotope-edited infrared spectroscopy[7]. Alternative methods have been also used that do not probe directly changes in H^+ concentration in the bulk phase, but the consequences of the proton release in terms of charge distribution within the protein that are reflected by electrochromic bandshifts, *e.g.* ref [6],or in terms of free enthalpy changes by time-resolved photothermal beam deflection, *e.g.* ref [2]. These time-resolved measurements evidenced the release of one proton per PSII preceding the electron transfer reaction associated with the $S_3^+Y_Z^\bullet \rightarrow S_0Y_Z$. All these data were obtained in PSII containing the natural cofactors Ca^{2+} and Cl^-. It has been shown earlier that the same applies in Sr-containing PSII[10]. To confirm that a fast proton release, preceding the $S_3^+Y_Z^\bullet \rightarrow S_0Y_Z$ electron transfer reaction, also occurs in Sr/Br-PSII, we have measured the kinetics of proton release in this PSII sample upon flash illumination with bromocresol purple as indicator dye. This could not be done with Sr/I-PSII owing to the difficulty to adjust the pH to 6.3 while keeping the concentration of Cl^- low enough to avoid a reverse I^-/Cl^- exchange and/or irreversible damages of the sample induced by a large I^- concentration. The experimental procedures involved are described in the Supplementary Methods section.

Supplementary Figure 4 shows the absorption changes at 575 nm[11], which are associated with changes in the protonation state of bromocresol purple, after the first three flashes given to a dark-adapted Sr/Br-PSII sample. At this wavelength, the unprotonated form of the dye has the largest extinction coefficient so that a light-induced decrease in absorbance reflects a H^+ release.

The time course of the absorption change measured after the first flash displays two components reflecting H^+ uptakes. The $t_{1/2}$ of the fast uptake phase is very similar to that of the reduction of the non-heme iron by $Q_A^{-\bullet}$ (~55 µs in Ca/Cl-PSII[12]), suggesting that the proton uptake is coupled to this electron transfer event. The slower proton uptake ($t_{1/2}$ is in the 10 ms time range) is observed also upon all the other flashes in the series. The origin of this slow phase will be further analysed below.

After both the 2nd and 3rd flash, a proton release is observed, followed by the above mentioned slow proton uptake. The rate constants of the proton release after the 2nd flash is close to the value expected from the literature[1,2]. After the 3rd flash, we observed, as previously reported for Ca/Cl PSII[13], a proton release developing in the sub ms time-range and thus being faster than the reduction of $Y_Z^\bullet$. We note here, that the amplitude of this fast proton release is similar

to that observed after the second flash, which is associated with the release of one H^+ per PSII. At this stage we can thus conclude qualitatively that in Sr/Br-PSII, as in the Ca/Cl-PSII case, the release of about one H^+ per PSII precedes the sequence of electron transfer reactions that lead to oxygen evolution.

In the following we will more quantitatively analyse these data to decipher the stoichiometry and the rate constants of the proton releases in the $S_3^+Y_Z$ to S_0Y_Z transition. In order to first calibrate the dye response in terms of H^+ release per PSII, we averaged the absorption changes associated with the 35^{th} to 40^{th} flash in a flash train (black symbols in Supplementary Figure 5). Under these conditions the S_i-states are scrambled and they thus all contribute equally upon each single flash, so that the H^+ release is expected to be 1-α per PSII (α being the miss parameter). As seen in Supplementary Figure 5, the kinetics of absorption changes associated with the flash induced pH changes displays two phases, one sub-ms phases associated with H^+ release followed by a slower H^+ uptake. The amplitude of the proton release phase nicely matches that of the fast H^+ release component observed after the third flash, thus confirming that it corresponds to the release of ~ 1 H^+ per PSII.

Supplementary Figure 5 also compares the averaged absorption changes measured upon the first four flashes (red points) to the average of the absorption changes measured upon the 35^{th} to 40^{th} flashes (black points). The kinetics shown in blue is the difference red-*minus*-black and reflects a proton uptake that is predominant on the first flashes and thus likely correspond to H^+ uptake associated with the reduction of the non-heme iron, which mainly occurs after the first flash. More importantly, at variance with the averaged kinetics in black (35^{th} to 40^{th} flashes) and red (1^{st} to 4^{th} flashes) the kinetics in blue displays no components developing in the ms time-range, thus showing that this component cancels out in the difference and can thus be considered as being constant upon each flash. We assign this slow H^+ uptake phase to the protonation of the added PPBQ.

This non-oscillating apparent proton uptake occurring in the 10 to 100 ms time range on all flashes was further characterized. To this aim, the proton release contribution in the averaged kinetics (35^{th} to 40^{th} flashes, full black circles in Supplementary Figures 5 and 6), was fitted. Since the average of the kinetics of the proton releases has by definition many phases, we used a stretched exponential. This has no physical meaning, but simply empirically provides a good fit of the decaying kinetics as shown by the continuous red line in Supplementary Figure 6. The uptake contribution (blue line in Supplementary Figure 6) was then obtained and by subtracting the empirical H^+ release time-course (red line in Supplementary Figure 6) from the experimental data.

We then subtracted this H^+ uptake contribution, which, as discussed above, evenly contribute upon each flashes and thereby obtained the H^+ release components after each flash in the series (shown in Supplementary Figure 7).

After the third flash one now clearly sees 2 components. A bi-exponential fit of these corrected data (Supplementary Figure 8) yields a half-time for the slow phase of 6.3 ms which is similar to the 7.2 ms value found for the electron transfer reaction associated with the $S_3^+Y_Z^\bullet \rightarrow S_0Y_Z$ transition in Sr/Br-PSII[10]. We note, however, that the fast phase ($t_{1/2}$ = 22 µs)

is faster than the data at 292 nm ($t_{1/2} \approx 200$ µs). Such an increase in the rate constant has been observed previously[13] and was attributed to a Bohr-effect that dependents on the dye concentration. Independent of this detail, these data unambiguously show that in Sr/Br-PSII samples two kinetically distinct protons are released in the $S_3^+Y_Z^\bullet \rightarrow S_3Y_Z^\bullet \rightarrow S_0Y_Z$ transition: one in the $S_3^+Y_Z^\bullet \rightarrow S_3Y_Z^\bullet$ transition and another one in the $S_3Y_Z^\bullet \rightarrow S_0Y_Z$ transition.

The stoichiometry of the proton release after each flash of the sequence can be deduced from the period 4 oscillations at 575 nm. First, the absorption (575 nm) detected 100 ms after each flash (see Supplementary Figure 4) in a series of 21 flashes was plotted in the Supplementary Figure 9. Calculation of the miss parameter (the first flash was not taken into account, for details see ref[14]) was performed assuming it was equal for all S-state transitions.

Second, the non-oscillating contribution of the proton uptake 100 ms after the flashes, which was determined in Supplementary Figure 6, was subtracted from the data points in Supplementary Figure 9. The points thus obtained are plotted in Supplementary Figure 10 as black symbols. Finally, the fitting procedure already described[14-16] was applied (continuous line in Supplementary Figure 10).

The pattern of the proton release resulting from the fitting procedure was found to be:

$S_0Y_Z \rightarrow S_1Y_Z$: 1.16

$S_1Y_Z \rightarrow S_2^+Y_Z$: 0.02

$S_2^+Y_Z \rightarrow S_3^+Y_Z$: 1.19

$S_3^+Y_Z \rightarrow S_0Y_Z$: 1.63

The pattern in Sr/Br-PSII is similar to those reported for Ca/Cl-PSII in the literature at pH 6.3 [6]. Thus, the Ca/Sr or Cl/Br substitution has little impact on the H^+ release stoichiometry associated with each S-state formation, and thus on the mechanism of water oxidation (for O_2 release see Supplementary Figure 3).

Supplementary Methods

Procedure for PSII preparations.

The Sr/Br-PSII sample was first washed once in 1 M Betaine, 15 mM $CaBr_2$, 15 mM $MgBr_2$, 40 mM Mes pH 6.3 and then several times in 1 M Betaine, 15 mM $CaBr_2$, 15 mM $MgBr_2$ previously adjusted to pH 6.3 with NaOH. The sample was then diluted into 1 M Betaine, 15 mM $CaBr_2$, 15 mM $MgBr_2$, 150 µM bromocresol purple adjusted to pH 6.3 with NaOH. The medium used to resuspend the PSII was prepared three days before the experiments to avoid a too strong pH drift during the experiment that otherwise occurs. After dark adaptation, 100 µM PPBQ (in DMSO) and 100 µM ferricyanide were added.

Absorption changes at 575 nm

Absorption changes were measured at 575 nm with a lab-built spectrophotometer[11] where the absorption changes are sampled at discrete times by short flashes. These flashes were provided by a neodymium:yttrium-aluminum garnet (Nd:YAG, 355 nm) pumped optical parametric oscillator, which produces monochromatic flashes (1 nm full-width at half-maximum) with a duration of 5 ns. Excitation was provided by a second neodymium:yttrium-aluminum garnet (Nd:YAG, 532 nm) pumped optical parametric oscillator, which produces monochromatic flashes at 700 nm (1 nm full-width at half-maximum) with a duration of 5 ns . The path length of the cuvette was 2.5 mm.

Supplementary References

1. Rappaport, F. & Lavergne, J. Coupling of electron and proton transfer in the photosynthetic water oxidase. *Biochim. Biophys. Acta* **1503,** 246-259 (2001).
2. Klauss, A., Haumann, M. & Dau, H. Alternating electron and proton transfer steps in photosynthetic water oxidation. *Proc. Natl. Acad. Sci. USA* **109,** 16035-16040 (2012).
3. Siegbahn, P. E. M. & Lundberg, M. The mechanism for dioxygen formation in PSII studied by quantum chemical methods. *Photochem. Photobiol. Sci.* **4,** 1035-1043 (2005).
4. Saphon, S. & Crofts, A. R. Protolytic reactions in photosystem II - new model for release of protons accompanying photooxidation of water. *Z Naturforsch C* **32,** 617-626 (1977).
5. Fowler, C. F. Proton evolution from photosystem II stoichiometry and mechanistic considerations. *Biochim. Biophys. Acta* **462,** 414-421 (1977).
6. Rappaport, F. & Lavergne, J. Proton release during successive oxidation steps of the photosynthetic water oxidation process - stoichiometries and pH-dependence. *Biochemistry* **30,** 10004-10012 (1991).
7. Suzuki, H., Sugiura, M. & Noguchi, T. Monitoring proton release during photosynthetic water oxidation in photosystem II by means of isotope-edited infrared spectroscopy. *J. Am. Chem. Soc.* **131,** 7849-7857 (2009).
8. Schlodder, E. & Witt, H. T. Stoichiometry of proton release from the catalytic center in photosynthetic water oxidation. *J. Biol. Chem.* **274,** 30387-30392 (1999).
9. Förster, V. & Junge, W. Stoichiometry and kinetics of proton release upon photosynthetic water oxidation. *Photochem. Photobiol.* **41,** 183-190 (1985).
10. Rappaport, F., Ishida, N., Sugiura, M. & Boussac, A. Ca^{2+} determines the entropy changes associated with the formation of transition states during water oxidation by photosystem II. *Energy Environ. Sci.* **4,** 2520-2524 (2011).
11. Beal, D., Rappaport, F. & Joliot, P. A new high-sensitivity 10-ns time-resolution spectrophotometric technique adapted to in vivo analysis of the photosynthetic apparatus. *Rev Sci Instrum* **70,** 202-207 (1999).
12. Boussac, A., Sugiura, M. & Rappaport, F. Probing the quinone binding site of Photosystem II from *Thermosynechococcus elongatus* containing either PsbA1 or PsbA3 as the D1 protein through the binding characteristics of herbicides. *Biochim. Biophys. Acta* **1807,** 119-129 (2011).
13. Junge, W., Haumann, M., Ahlbrink, R., Mulkidjanian, A. & Clausen, J. Electrostatics and proton transfer in photosynthetic water oxidation. *Philos. Trans. R. Soc Lond., B* **357,** 1407-1417 (2002).
14. Ishida, N. *et al.* Biosynthetic exchange of bromide for chloride and strontium for calcium in the photosystem II oxygen-evolving enzymes. *J. Biol. Chem.* **283,** 13330-13340 (2008).
15. Lavergne, J. Absorption changes of photosystem II donors and acceptors in algal cells. *FEBS Letters* **173,** 9-14 (1984).
16. Lavergne, J. Improved UV-visible spectra of S-state transitions in the photosynthetic oxygen evolving system. *Biochim. Biophys. Acta* **1060,** 175-188 (1991).